

# Additivity of Dilantin and Vinblastine Inhibitory Effects on Microtubule Assembly<sup>1</sup>

Sharon Lobert,<sup>2</sup> Jeffrey W. Ingram, and John J. Correia

School of Nursing [S. L.] and Department of Biochemistry [S. L., J. W. I., J. J. C.], University of Mississippi Medical Center, Jackson, Mississippi 39216

## ABSTRACT

Dilantin (phenytoin) is a commonly used antiepileptic agent that is known to decrease conductance of sodium and calcium ions and delay outward potassium currents. Separate from its antiseizure activity, dilantin interferes with microtubule protein polymerization. It induces metaphase arrest and potentiates the effects of the antimetabolites vincristine and vinblastine in cell culture. We show here by fluorescence binding studies that dilantin interacts directly with tubulin at a low affinity site [ $K_a = 3.5 (\pm 2.5) \times 10^3 \text{ M}^{-1}$ ;  $K_d = 286 \mu\text{M}$ ]. We quantitatively examined the effect of dilantin on bulk microtubule formation and found that the drug raises the critical concentration for microtubule polymerization in 2 M glycerol identically in the presence or absence of vinblastine. The change in free energy for microtubule polymerization attributable to 400  $\mu\text{M}$  dilantin [ $\Delta\Delta G = 117 (\pm 28) \text{ cal/mol}$ ] is additive with vinblastine effects. Under the same conditions, mean microtubule lengths are  $7.7 \pm 4.3 \mu\text{m}$  ( $n = 558$ ) and  $7.4 \pm 4.0 \mu\text{m}$  ( $n = 477$ ) in the presence or absence of dilantin, respectively. Dilantin has no effect on vinblastine-induced tubulin spiral formation, as measured by sedimentation velocity. Our data suggest that the mechanism for the antimicrotubule effects of dilantin involves sequestration of tubulin heterodimers in 1:1 drug:tubulin complexes that do not participate in tubulin polymerization. The dilantin binding site is distinct from the *Vinca* binding site, and these independent binding modes account for the additive effects *in vitro*. The sequestration of tubulin heterodimers could explain the combined drug synergy in cell cultures if it disrupted interactions with proteins that regulate microtubule dynamics and/or cell cycle events.

## INTRODUCTION

For over 30 years, *Vinca* alkaloids (vinblastine, vincristine, and more recently, vinorelbine) have played a major role in cancer chemotherapy. They cause mitotic arrest by interacting with tubulin heterodimers and mitotic spindle microtubules. *Vinca* alkaloids inhibit the polymerization of tubulin into microtubules, and it has been suggested that *in vivo Vincas* act at the ends of microtubules and diminish an essential aspect of cell division, dynamic instability (1, 2). *Vinca* alkaloids produce their antitumor effects by halting cell division at metaphase; however, their efficacy is limited by their primary toxicities. *Vinca* binding to tubulin is linked to spiral formation, a phenomenon proposed to be significant for drug action and toxicity (3–6). Vincristine and vinblastine are very similar structurally (substitution of a formyl group for a methyl group in vincristine compared with vinblastine), but the dose-limiting toxicity for vincristine is neurotoxicity, whereas bone marrow toxicity limits the use of vinblastine (reviewed in Ref. 7). The reasons for these different tissue-specific toxic effects are not known. Chemotherapy regimens with drug combinations that reduce the toxic effects of *Vincas* will enhance their antineoplastic usefulness, and thus the potential for therapeutic strategies using multiple antimicrotubule agents with different modes

of action is under investigation (8–11). The combination of dilantin (phenytoin) and vinblastine is reported to be in Phase I trials (12).

Dilantin (phenytoin) is commonly used for its antiepileptic properties. It stabilizes membranes in neurons and cardiac myocytes (13) and is known to decrease conductance of sodium and calcium ions and delay outward potassium currents. Some of the effects of dilantin on neuronal synaptic signaling may be due indirectly to its effects on microtubules. Dilantin inhibits a  $\text{Ca}^{2+}$ -calmodulin tubulin kinase (14), thereby diminishing phosphorylation that occurs uniquely on neuron-specific  $\beta$ -class III tubulin. Thus, the inactivation of the tubulin kinase may affect utilization of tubulin at synaptic terminals. Separate from its action as an antiseizure agent, dilantin is known to interfere with microtubule polymerization (15–17). In cells, it also induces metaphase arrest, suggesting it could affect mitotic spindles. It weakly displaces the antimetabolite colchicine from its tubulin binding site, but unlike colchicine, it was not shown to depolymerize microtubules. Because colchicine binds to tubulin at a site separate from the *Vinca* alkaloid binding site, this result suggests that dilantin also does not bind at the *Vinca* alkaloid binding site. Note that these previous studies were carried out with purified microtubule protein (tubulin plus MAPs<sup>3</sup>). Although inhibition of tubulin polymerization was shown to be necessary for metaphase arrest by dilantin (16), it is not known whether MAPs are involved in its antimicrotubule activity. MAPs are known to stabilize microtubules. During cell division, MAPs are hyperphosphorylated and released from microtubules, thereby increasing mitotic spindle dynamics.

Most recently, dilantin was shown to enhance the effects of the antimetabolites vincristine and vinblastine in cell culture (12, 18). This enhancement was described as “synergy” because the combined effect was greater than that produced by either vinblastine or dilantin alone, and the dilantin concentrations in these experiments were much lower than those needed to inhibit microtubule polymerization. It was shown that dilantin does not significantly affect intracellular vincristine concentrations, and thus, the synergy was not due to diminishing drug efflux caused by P-glycoprotein. An increase in apoptotic response was observed when cell cultures are exposed to both vinblastine and dilantin compared with single agents (12). The origin of this dilantin-*Vinca* alkaloid synergy remains uncertain.

The goal of the work described here was to evaluate and quantify the molecular basis for combined vinblastine and dilantin therapy through *in vitro* experiments. Comparisons at the drug receptor level are essential for understanding the clinical efficacy and toxicity of these drugs in combination. A synergistic interaction in cell culture suggests a cooperative interaction at the molecular level. Our data indicate that effects of combined dilantin and vinblastine on microtubule assembly are additive and not cooperative. Dilantin does not alter vinblastine-induced tubulin spiral size or microtubule length. Our data suggest that *in vitro* dilantin enhances vinblastine effects by sequestering tubulin in liganded heterodimers that do not participate in microtubule polymerization. This sequestration of tubulin heterodimers could explain the combined drug synergy in cell cultures if it disrupted interactions with proteins that regulate microtubule dynamics and/or cell cycle events.

Received 3/11/99; accepted 8/4/99.

The costs of publication of this article were defrayed in part by the payment of page charges. This article must therefore be hereby marked *advertisement* in accordance with 18 U.S.C. Section 1734 solely to indicate this fact.

<sup>1</sup> This work was supported by a grant from the Oncology Nursing Foundation/Bristol Myers-Squibb (to S. L. and J. J. C.) and NIH Grant NR04780 (to S. L. and J. J. C.).

<sup>2</sup> To whom requests for reprints should be addressed, at University of Mississippi Medical Center, School of Nursing and Department of Biochemistry, 2500 North State Street, Jackson, Mississippi 39216. Phone: (601) 984-1852; E-mail: slobert@son.umsmed.edu.

<sup>3</sup> The abbreviations used are: MAP, microtubule-associated protein; PC-tubulin, MAP-free phosphocellulose purified tubulin; MTP, microtubule protein; Pipes, piperazine-*N,N'*-bis(2-ethanesulfonic acid).

## MATERIALS AND METHODS

**Reagents.** Deionized (Nanopure) water was used in all experiments. DMSO,  $\text{MgSO}_4$ , EGTA, GTP (type II-S), glycerol, Pipes, podophyllotoxin, vinblastine sulfate, and dilantin (5,5 diphenylhydantoin) were purchased from Sigma Chemical Co. Sephadex G-50 was from Pharmacia.

**Tubulin Purification.** MTP from porcine brain was obtained by two cycles of warm-cold polymerization-depolymerization. Purified tubulin (PC-tubulin) free of MAPs was obtained by the addition of a final phosphocellulose chromatography step to separate tubulin from MAPs (19, 20). Protein concentrations were determined spectrophotometrically ( $\epsilon_{278} = 1.2 \text{ l/g-cm}$ ; Ref. 21).

**Critical Concentrations.** PC-tubulin (1–3.5 mg/ml) was polymerized in 100 mM Pipes (pH 6.9), 1 mM  $\text{MgSO}_4$ , 2 mM EGTA, 1 mM GTP, and 2 M glycerol. MTP (0.6–3 mg/ml) was polymerized in the same buffer without glycerol. Microtubule formation was monitored using a Gilford Response II UV-VIS scanning spectrophotometer equipped with a cooling Peltier cell holder. Prior to polymerization, samples were degassed on ice for 30 min, and baseline data were collected at 4°C and 350 nm. The temperature was increased to 37°C, and solutions were monitored at 350 nm for 45 min. Solutions were cooled to 0°C, and a second baseline was recorded. The change in absorbance was plotted *versus* tubulin concentration after subtracting the second baseline from the plateau absorbance at 45 min. The critical concentration was determined from the X-intercept of the linear regression fits of the data. Critical concentrations were determined by combining the data from two or more independent experiments. Three different tubulin preparations were used in these experiments. To determine the effect of drugs on the critical concentrations, experiments were carried out in the presence or absence of dilantin (200, 400, and 600  $\mu\text{M}$ ) or vinblastine (0.5, 1, and 1.5  $\mu\text{M}$ ). Experiments with combined 400  $\mu\text{M}$  dilantin plus vinblastine (0.5, 1, and 1.5  $\mu\text{M}$ ) were also performed. Dilantin stocks were made up in DMSO at 20 mM; therefore, corresponding amounts of DMSO were added to control and experimental solutions. To evaluate the mechanism of combined vinblastine and dilantin effects, similar experiments were carried out with podophyllotoxin (500 nM and 1  $\mu\text{M}$ ), an antimicrotubule drug that is known to sequester tubulin in a 1:1 drug:heterodimer complex. Podophyllotoxin concentrations were determined using the extinction coefficient:  $\epsilon_{\text{water}, 290} = 4400 \text{ M}^{-1} \text{ cm}^{-1}$  (22).

**Fluorescence Binding Experiments.** Dilantin (80–630  $\mu\text{M}$ ) was added in increments to PC-tubulin (2  $\mu\text{M}$ ) in 10 mM Pipes (pH 6.9), 2 mM EGTA, 1 mM  $\text{MgSO}_4$ , 0.05 mM GTP, and 2% DMSO at 25°C, and relative intrinsic fluorescence of tubulin was monitored in an SLM Aminco Bowman Series 2 Luminescence Spectrometer using an excitation wavelength of 286 nm and emission wavelength of 326 nm. The data were corrected empirically for drug absorbance and inner filter effects using a tryptophan solution at a concentration equivalent to the molar concentration of tryptophan at the experimental tubulin concentration (23). When dilantin is added to tubulin solutions, the relative fluorescence increases. The change in fluorescence can be plotted *versus* dilantin concentration and the data fit by least squares to directly obtain the binding constant using software developed in Fital (MTR software, Toronto, Canada). These experiments were limited by the magnitude of the signal at low dilantin concentrations and the solubility of dilantin at high concentrations.

**Microtubule Length Distributions.** PC-tubulin samples (2 mg/ml) were prepared on ice in the presence or absence of 400  $\mu\text{M}$  dilantin in 100 mM Pipes (pH 6.9), 2 M glycerol, 1 mM GTP, 2 mM EGTA, and 1 mM  $\text{MgSO}_4$ . Samples were warmed to 37°C for 30 min and then prepared for electron microscopy. The method used for glutaraldehyde fixation and negative staining with uranyl acetate has been described previously (3). Grids were examined and photographed using a Zeiss EM 912 Omega electron microscope. Microtubule lengths were measured from photographs by two independent observers using a digitizing tablet and Sigma Scan software (Jandel Scientific; SigmaScan Pro 3.0). Only microtubules with both ends clearly visible were measured. At least 470 microtubules were measured for each data set.

**Sedimentation Velocity Experiments.** Vinblastine-induced tubulin spiral formation was studied in the presence or absence of dilantin by sedimentation velocity as described previously (3). PC-tubulin was equilibrated using spun Sephadex G-50 columns into 100 mM Pipes (pH 6.9), 2 M glycerol, 2 mM EGTA, 1 mM  $\text{MgSO}_4$  and 0.05 mM GTP in the presence or absence of vinblastine or vinblastine plus 400  $\mu\text{M}$  dilantin. To assure that the protein was equilibrated in the glycerol buffer, two sequential spun columns were used for

each sample. The free vinblastine concentration (0.5–70  $\mu\text{M}$ ) was obtained from the known drug concentration in the equilibration buffer. Sedimentation studies were done in a Beckman Optima XLA analytical ultracentrifuge equipped with absorbance optics and an An60 Ti rotor. Temperature was calibrated by the method of Liu and Stafford (24). Samples were spun at 37°C and appropriate speeds. Velocity data were collected at 278 nm and at a spacing of 0.002 cm with one average in a continuous scan mode. Data were analyzed using software (DCDT) provided by Dr. Walter Stafford (Boston Biomedical Research Institute) to generate a distribution of sedimentation coefficients,  $g(s)$ , and weight average sedimentation coefficients,  $\bar{s}_w$ , as described previously (3). These data were corrected for empirically determined density (Anton Paar DMA 500 density meter) and viscosity at 37°C and plotted as weight average  $\bar{s}_{20,w}$  *versus* free drug. Models with two or four binding constants were used to fit the data with the nonlinear least squares program Fital (MTR Software, Toronto, Canada), modified to include the appropriate fitting functions. In these models,  $K_1$  is the affinity of drug for tubulin heterodimers,  $K_2$  is the affinity of liganded-heterodimers for spiral polymers,  $K_3$  is the affinity of drug for polymers, and  $K_4$  is the association constant for unliganded-tubulin heterodimers. The method for curve fitting to obtain binding affinities has been described previously (3).

## RESULTS

**Dilantin Inhibition of Tubulin Polymerization.** PC-tubulin polymerization into microtubules in 2 M glycerol was monitored by spectroscopy at 350 nm after increasing the temperature from 4°C to 37°C. Fig. 1 shows the dilantin-dependent decrease in turbidity or microtubule mass in the presence of 200, 400, and 600  $\mu\text{M}$  dilantin. Fig. 2 shows the dilantin enhancement of vinblastine-induced inhibition of microtubule formation. The presence of 400  $\mu\text{M}$  dilantin significantly reduces the polymer mass over and above the effect of 0.5 or 1  $\mu\text{M}$  vinblastine. Note that 400  $\mu\text{M}$  dilantin is a clinically achievable intracellular concentration because therapeutic plasma levels are 55–110  $\mu\text{M}$  dilantin, and the drug is known to be concentrated 4–7-fold in cells (25).

To quantitatively examine the effect of dilantin on microtubule formation, turbidity was monitored in the presence and absence of drug over a range of tubulin concentrations. The critical concentration or free heterodimer concentration was determined from the X-intercept of plots of tubulin concentration *versus* change in absorbance (Fig. 3). The presence of 400  $\mu\text{M}$  dilantin increases the critical concentration from 0.310 ( $\pm 0.078$ ) to 0.375 ( $\pm 0.075$ )

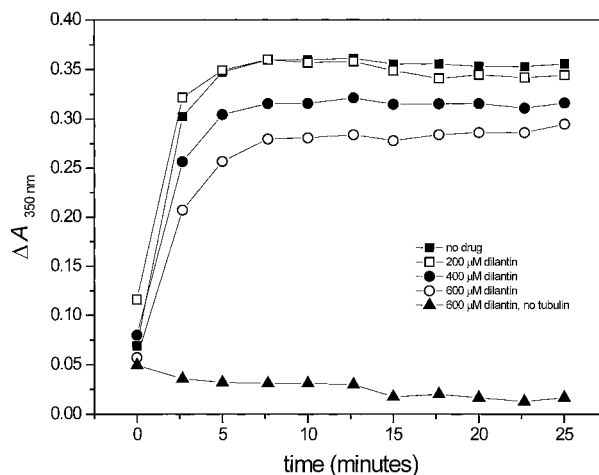


Fig. 1. Microtubule polymerization in the presence of dilantin. PC-tubulin (1.8 mg/ml) in polymerization buffer (see "Materials and Methods") was warmed to 37°C, and turbidity was monitored at 350 nm. After 30 min, the solutions were cooled to 4°C to obtain a baseline. The plots show the change in turbidity after correcting the data for the baseline absorbance. ■, no dilantin; □, 200  $\mu\text{M}$  dilantin; ●, 400  $\mu\text{M}$  dilantin; ○, 600  $\mu\text{M}$  dilantin; ▲, 600  $\mu\text{M}$  dilantin, no tubulin.

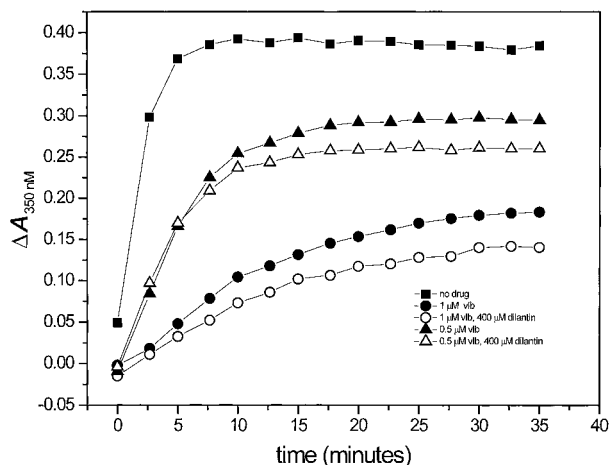


Fig. 2. Microtubule polymerization in the presence of dilantin and vinblastine. PC-tubulin was polymerized, and the change in turbidity was determined as described in Fig. 1. ■, no drug; ▲, 0.5  $\mu\text{M}$  vinblastine; △, 0.5  $\mu\text{M}$  vinblastine and 400  $\mu\text{M}$  dilantin; ●, 1  $\mu\text{M}$  vinblastine; ○, 1  $\mu\text{M}$  vinblastine and 400  $\mu\text{M}$  dilantin.

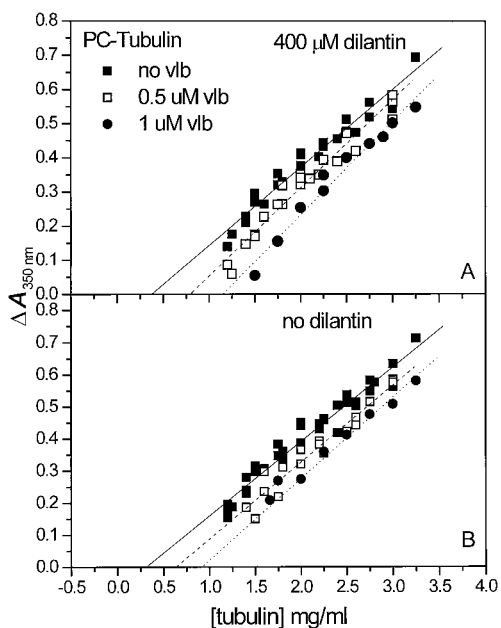


Fig. 3. Determination of critical concentrations for PC-tubulin polymerization. PC-tubulin at various concentrations (1–3.5 mg/ml) was polymerized as described in Figs. 1 and 2. The baselines at 4°C were determined and subtracted from the plateau absorbance at 45 min to obtain the change in absorbance. The data were fit by linear regression, and critical concentration was determined from the X-intercept. ■, no vinblastine; □, 0.5  $\mu\text{M}$  vinblastine; ●, 1  $\mu\text{M}$  vinblastine. A, 400  $\mu\text{M}$  dilantin; B, no dilantin. Note that these studies involved multiple experiments with more than one tubulin preparation. Individual differences in tubulin preparations contribute to the scatter in the data.

mg/ml (Table 1). Experiments were carried out in the presence of 0.5, 1.0, or 1.5  $\mu\text{M}$  vinblastine with and without 400  $\mu\text{M}$  dilantin. (The 1.5  $\mu\text{M}$  vinblastine data were omitted from Fig. 3 for clarity of presentation.) As shown in Fig. 3 and summarized for all data in Table 1, dilantin increases the critical concentration for microtubule formation in the presence of vinblastine.

To determine whether MAPs might contribute to the dilantin enhancement of *Vinca* alkaloid-induced cytotoxicity observed in cell culture, turbidity experiments were carried out with twice-cycled MTP in the presence or absence of 400  $\mu\text{M}$  dilantin (Fig. 4). The critical concentrations determined in these experiments are given in Table 1. The critical concentrations were 0.096 and 0.121 mg/ml in

the absence and presence of 400  $\mu\text{M}$  dilantin. The magnitude of the difference in critical concentrations is similar to that found with PC-tubulin, 21–26% increase. Experiments were also carried out in the presence of 1  $\mu\text{M}$  vinblastine with and without 400  $\mu\text{M}$  dilantin. Dilantin increased the critical concentration for MTP polymerization in the presence of vinblastine (Table 1). This effect is somewhat smaller than that found with PC-tubulin. Note that, for MTP, the slopes of the change in turbidity plots (Fig. 4) are also different in the absence or presence of dilantin. This slope change is not found with PC-tubulin and suggests that dilantin induces a redistribution of tubulin and MAPs into smaller oligomers that scatter light differently than microtubules.

Tables 2 and 3 show a series of thermodynamic cycles representing the energetics of the effects of dilantin, vinblastine, and combined vinblastine plus dilantin on microtubule formation. The equilibrium constant for microtubule propagation,  $K_p$ , is obtained from the reciprocal of the critical concentration and used to calculate free energy ( $\Delta G = -RT \ln K_p$ ) for each condition. The change in free energy,  $\Delta \Delta G$ , is then calculated between conditions. The inhibition of microtubule assembly attributable to a fixed concentration of dilantin is within error constant and additive under all conditions studied. The average  $\Delta \Delta G$  due to the presence of 400  $\mu\text{M}$  dilantin is 117 ( $\pm 28$ ) cal/mol. This means the inhibitory effect of dilantin is the same in the presence and absence of vinblastine. For example in the absence of vinblastine, the  $\Delta G$  for microtubule assembly is  $-7.81 \times 10^3$  cal/mol

Table 1 Critical concentrations

	mg/ml ( $\pm$ SD)
PC-tubulin	
No drug	0.310 ( $\pm$ 0.078)
400 $\mu\text{M}$ dilantin	0.375 ( $\pm$ 0.075)
0.5 $\mu\text{M}$ vlb <sup>a</sup>	0.634 ( $\pm$ 0.151)
0.5 $\mu\text{M}$ vlb, 400 $\mu\text{M}$ dilantin	0.794 ( $\pm$ 0.103)
1.0 $\mu\text{M}$ vlb	0.914 ( $\pm$ 0.230)
1.0 $\mu\text{M}$ vlb, 400 $\mu\text{M}$ dilantin	1.150 ( $\pm$ 0.140)
1.5 $\mu\text{M}$ vlb	1.064 ( $\pm$ 0.311)
1.5 $\mu\text{M}$ vlb, 400 $\mu\text{M}$ dilantin	1.226 ( $\pm$ 0.225)
MTP	
No drug	0.096 ( $\pm$ 0.039)
400 $\mu\text{M}$ dilantin	0.121 ( $\pm$ 0.005)
1.0 $\mu\text{M}$ vlb	0.579 ( $\pm$ 0.117)
1.0 $\mu\text{M}$ vlb, 400 $\mu\text{M}$ dilantin	0.618 ( $\pm$ 0.077)

<sup>a</sup> vlb, vinblastine.

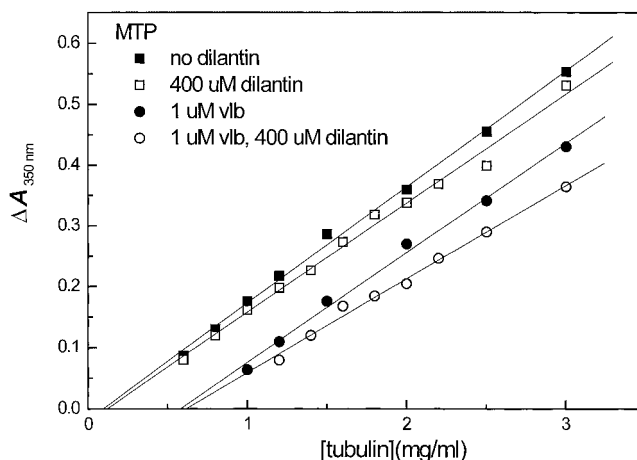


Fig. 4. Determination of critical concentrations for MTP polymerization. MTP at various concentrations (0.6–3.0 mg/ml) was polymerized as described in Figs. 1 and 2. The baselines at 4°C were determined and subtracted from the plateau absorbance at 45 min to obtain the change in absorbance. The data were fit by linear regression, and critical concentration was determined from the X-intercept. ■, no dilantin; □, 400  $\mu\text{M}$  dilantin; ●, 1  $\mu\text{M}$  vinblastine; ○, 1  $\mu\text{M}$  vinblastine, 400  $\mu\text{M}$  dilantin.

Table 2 Free energy for microtubule polymerization (PC-tubulin, 37°C)<sup>a</sup>

No dilantin	$\Delta\Delta G$	Dilantin
No drug	→	400 $\mu\text{M}$ dilantin
$\Delta G = -7.81 \times 10^3$ cal	$\Delta\Delta G = 110$ cal	$\Delta G = -7.70 \times 10^3$ cal
↓ $\Delta\Delta G = 440$ cal		$\Delta\Delta G = 470$ cal ↓
0.5 $\mu\text{M}$ vinblastine	→	0.5 $\mu\text{M}$ vinblastine, 400 $\mu\text{M}$ dilantin
$\Delta G = -7.37 \times 10^3$ cal	$\Delta\Delta G = 139$ cal	$\Delta G = -7.23 \times 10^3$ cal
↓ $\Delta\Delta G = 224$ cal		$\Delta\Delta G = 224$ cal ↓
1.0 $\mu\text{M}$ vinblastine	→	1.0 $\mu\text{M}$ vinblastine, 400 $\mu\text{M}$ dilantin
$\Delta G = -7.15 \times 10^3$ cal	$\Delta\Delta G = 139$ cal	$\Delta G = -7.01 \times 10^3$ cal
↓ $\Delta G = 100$ cal		$\Delta G = 40$ cal ↓
1.5 $\mu\text{M}$ vinblastine	→	1.5 $\mu\text{M}$ vinblastine, 400 $\mu\text{M}$ dilantin
$\Delta G = -7.05 \times 10^3$ cal	$\Delta\Delta G = 80$ cal	$\Delta G = -6.97 \times 10^3$ cal

<sup>a</sup> The free energy was calculated from the  $K_p$ , equilibrium constant for microtubule polymerization, determined from turbidity experiments.  $\Delta G$  is the free energy for the addition of a tubulin heterodimer to a microtubule, and  $\Delta\Delta G$  is the change in free energy for microtubule polymerization due to the presence of dilantin, vinblastine, or both.

Table 3 Free energy for microtubule polymerization (MTP, 37°C)<sup>a</sup>

No dilantin	$\Delta\Delta G$	Dilantin
No drug	→	400 $\mu\text{M}$ dilantin
$\Delta G = -8.53 \times 10^3$ cal	$\Delta\Delta G = 140$ cal	$\Delta G = -8.39 \times 10^3$ cal
↓ $\Delta\Delta G = 1100$ cal		$\Delta\Delta G = 1000$ cal ↓
1.0 $\mu\text{M}$ vinblastine	→	1.0 $\mu\text{M}$ vinblastine, 400 $\mu\text{M}$ dilantin
$\Delta G = -7.43 \times 10^3$ cal	$\Delta\Delta G = 40$ cal	$\Delta G = -7.39 \times 10^3$ cal

<sup>a</sup> The free energy was calculated from the  $K_p$ , equilibrium constant for microtubule polymerization, determined from turbidity experiments.  $\Delta G$  is the free energy for the addition of a tubulin heterodimer to a microtubule, and  $\Delta\Delta G$  is the change in free energy for microtubule polymerization due to the presence of dilantin, vinblastine, or both.

(Table 2). The addition of 400  $\mu\text{M}$  dilantin increases the  $\Delta G$  to  $-7.70 \times 10^3$  cal/mol, corresponding to a change in free energy for polymer formation,  $\Delta\Delta G$ , of 110 cal/mol. In the presence of 0.5  $\mu\text{M}$  vinblastine, the  $\Delta G$  for microtubule formation is  $-7.37 \times 10^3$  cal/mol, and the addition of 400  $\mu\text{M}$  dilantin raises the  $\Delta G$  to  $-7.23 \times 10^3$  cal/mol. Thus, the  $\Delta\Delta G$  attributable to dilantin in the presence of 0.5  $\mu\text{M}$  vinblastine is 139 cal/mol. When 1.0  $\mu\text{M}$  or 1.5  $\mu\text{M}$  vinblastine is present,  $\Delta\Delta G$  attributable to dilantin is 139 and 80 cal/mol, respectively. Increasing to 1.5  $\mu\text{M}$  vinblastine, the  $\Delta\Delta G$  for the addition of both drugs is reduced, possibly because microtubule ends are saturated by drug at these concentrations and therefore, the drug inhibitory free energy is diminished. For MTP, the  $\Delta\Delta G$  value is similar, although with a larger SD, 90 ( $\pm 50$ ) cal/mol (Table 3). If the activities of the two drugs were synergistic at the receptor level, rather than additive, the  $\Delta\Delta G$  for the effect of each drug would be greater when the second drug is present. In other words, synergy or cooperativity would produce corresponding branches of the thermodynamic cycle with unequal  $\Delta\Delta G$  values. Additivity is necessarily also apparent when the effect of vinblastine is examined (Table 2). At 0.5  $\mu\text{M}$  vinblastine, the  $\Delta\Delta G$  is 440 cal/mol versus 470 cal/mol in the absence or presence of dilantin. Increasing to 1  $\mu\text{M}$  vinblastine, the  $\Delta\Delta G$  is 224 cal/mol, both in the absence or presence of dilantin. It is noteworthy that the additive contribution of dilantin to the vinblastine inhibition of microtubule polymerization can be accounted for quantitatively by a direct interaction of the drugs with tubulin, not requiring an interaction with MAPs.

**Direct Dilantin-Tubulin Binding by Fluorescence.** The intrinsic tubulin difference fluorescence signal was found to increase with increasing dilantin concentrations, suggesting a conformational change in tubulin that is associated with drug binding (Fig. 5). At drug concentrations  $>630 \mu\text{M}$ , dilantin was insoluble, thereby limiting the maximum drug concentrations that could be studied. The fluorescence difference data, after correction for inner filter effects, were fit directly, assuming a single site to obtain the equilibrium binding constant,  $K_a = 3.5 (\pm 2.5) \times 10^3 \text{ M}^{-1}$  ( $K_d = 286 \mu\text{M}$ ). This weak binding affinity supports the turbidity studies where inhibition of microtubule

polymerization occurred at dilantin concentrations between 200 and 600  $\mu\text{M}$ .

**Dilantin Effect on Microtubules by Electron Microscopy.** To begin to understand the mechanism whereby dilantin inhibits microtubule polymerization, electron microscopy was used to examine length distributions in the presence and absence of the drug. Microtubule formation occurs via a nucleation phase, followed by elongation of polymers. Longer microtubules in the presence of dilantin would suggest that fewer nuclei form while elongation is unimpeded. Tubulin was polymerized under the same conditions used in the turbidity experiments, and samples for electron microscopy were made as described in "Materials and Methods." We found no significant difference in microtubule length in the presence or absence of 400  $\mu\text{M}$  dilantin, 7.70 ( $\pm 4.27$ ;  $n = 558$ ) and 7.40 ( $\pm 4.0$ ;  $n = 477$ )  $\mu\text{m}$  (Fig. 6). Thus, the decrease in total microtubule mass observed in the turbidity experiments is not due to impaired microtubule growth,

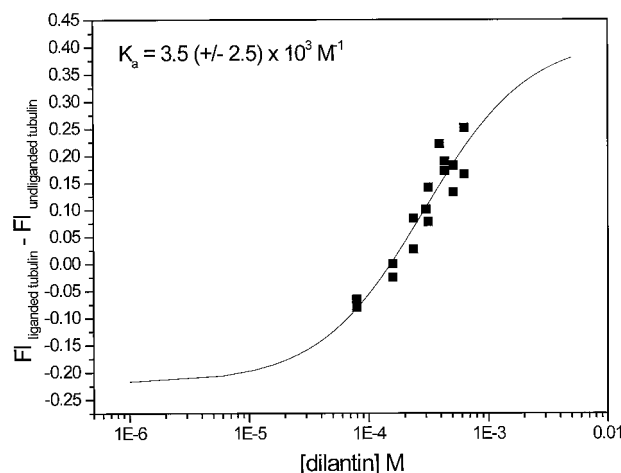


Fig. 5. Dilantin binding to PC-tubulin. Dilantin, 80–630  $\mu\text{M}$ , was added in successive increments to 2  $\mu\text{M}$  PC-tubulin, and the fluorescence was monitored using an excitation wavelength of 286 nm and emission wavelength of 326 nm, as described in "Materials and Methods." The change in tubulin fluorescence with increasing dilantin concentrations is plotted. Note that the experimental conditions are limited because of drug solubility and magnitude of the signal. Solid line, least squares fit of the data to obtain the equilibrium constant:  $K_a = 3.5 (\pm 2.5) \times 10^3 \text{ M}^{-1}$ .

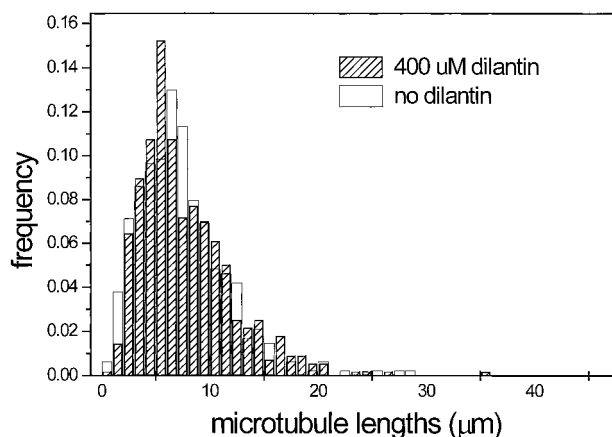


Fig. 6. Microtubule length distributions in the presence or absence of 400  $\mu\text{M}$  dilantin. PC-tubulin (2 mg/ml) was polymerized for 30 min as described in "Materials and Methods" in the absence of drug ( $\square$ ,  $n = 477$ ) or presence of 400  $\mu\text{M}$  dilantin ( $\square$ ,  $n = 558$ ). Samples were fixed in 1% glutaraldehyde and stained with 1% uranyl acetate. Microtubule lengths were measured from photographs using a digitizing tablet by two independent observers. No significant difference in mean microtubule lengths was found: mean lengths, 7.70 ( $\pm 4.27$ ) and 7.40 ( $\pm 4.0$ )  $\mu\text{m}$  in the presence and absence of dilantin, respectively.

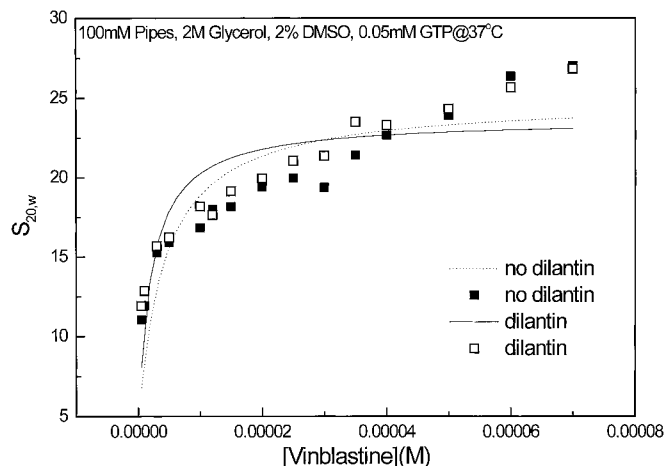


Fig. 7. Effect of dilantin on vinblastine-induced spiral formation by sedimentation velocity. PC-tubulin ( $2 \mu\text{M}$ ) was equilibrated into 100 mM Pipes (pH 6.9), 2 M glycerol, 2% DMSO, 1 mM  $\text{MgSO}_4$ , 2 mM EGTA, and 50  $\mu\text{M}$  GTP with vinblastine concentrations ranging from 0.5 to 70  $\mu\text{M}$  in the presence ( $\square$ ) or absence ( $\blacksquare$ ) of 400  $\mu\text{M}$  dilantin, and sedimentation velocity experiments were carried out at 37°C as described in “Materials and Methods.” Lines, best fits of the data using the ligand-mediated model. Solid line, data in the presence of dilantin; dotted line, data in the absence of dilantin. No significant difference in binding affinities were found. The binding affinities for vinblastine obtained from ligand-mediated fits of these data in the absence or presence of dilantin are:  $K_1 = 1.2 \times 10^5 (\pm 0.3)$  and  $1.7 \times 10^5 (\pm 0.4) \text{ M}^{-1}$ ;  $K_2 = 1.4 \times 10^7 (\pm 0.2)$  and  $1.2 \times 10^7 (\pm 0.2) \text{ M}^{-1}$ . Similar relative differences were found with combined model fits of the data.

suggesting that dilantin does not directly interfere with polymerization by binding to microtubules.

**Dilantin Effect on Vinblastine-induced Spiral Formation.** Vinblastine binding to tubulin is linked to tubulin spiral formation (3); therefore, the spirals are equilibrium polymers that contribute to the effect of vinblastine on microtubule dynamics. We investigated the interaction of dilantin with vinblastine-induced tubulin spirals to determine whether dilantin enhancement of vinblastine inhibition of microtubule formation was attributable to stabilization of spirals. Sedimentation velocity was used to assess spiral size over a range of vinblastine concentrations (0.5–70  $\mu\text{M}$ ) in the presence or absence of 400  $\mu\text{M}$  dilantin. The experiments were carried out in the same buffer as the turbidity experiments except, because of limitations of absorbance optics in the XLA analytical ultracentrifuge, GTP was 50  $\mu\text{M}$  instead of 1 mM. The  $\bar{s}_{20,w}$  values obtained from these experiments were plotted versus drug concentrations (Fig. 7) and fit to obtain binding constants. There was no significant difference in the equilibrium constants determined from control and experimental conditions. The overall binding affinities,  $K_1K_2$ , when data were fit with the ligand-mediated model were  $1.6 \times 10^{12}$  and  $2.2 \times 10^{12} \text{ M}^{-2}$ , in the absence or presence of dilantin. Similarly, no difference was found when data were fit with the combined model  $K_1K_2$  (data not shown). Thus, we conclude that the dilantin enhancement of the vinblastine inhibition of microtubule formation is not attributable to stabilization of vinblastine-induced tubulin spirals. Because dilantin binds directly to tubulin (Fig. 5), these data require that by microscopic reversibility, dilantin also binds to *Vinca*-induced spirals but neither stabilizes nor destabilizes them.

## DISCUSSION

Synergy and additivity of drug effects are complex concepts, having definitions that vary depending upon whether investigations occur at the whole animal, cellular, or drug-receptor level. In animal studies or clinical trials, quantification of combined drug interactions is complicated by the observation that for each drug, nonlinear dose

response and toxicity must be considered (26). For drugs that act at the same receptor, such as the antimetabolic agents, both the combined activity and underlying mechanisms can be investigated quantitatively *in vitro*. Changes in free energy distinguish synergy or cooperativity from additivity. Although interactions at a unique receptor may not completely explain the drug effects *in vivo*, a quantitative understanding of these effects helps to delineate the significant intracellular events.

The mechanism of action of antimetabolic agents has been the subject of intense investigation. These drugs disrupt microtubule dynamics essential for mitotic spindle activity. At stoichiometric concentrations, they either stabilize tubulin in microtubules (*e.g.*, Taxol) or induce depolymerization of microtubules (*e.g.*, vinblastine). In the work described here, we were able to quantify drug-receptor activity in terms of free energy, and we draw conclusions regarding the mechanisms underlying the combined drug effects. We demonstrate that dilantin is a tubulin-binding drug, albeit with weak affinity,  $K_d = 286 \mu\text{M}$ . This is the first report showing that MAPs are not required for the antimicrotubule activity of the drug. The effects on tubulin polymerization occur at dilantin concentrations between 200 and 600  $\mu\text{M}$  and, therefore, can be attributed to the weak binding of dilantin to tubulin. These dilantin concentrations are physiologically significant because the drug is concentrated intracellularly 4–7-fold (25), and plasma concentrations of 55–110  $\mu\text{M}$  are clinically achievable. Enhancement of vinblastine and vincristine cytotoxicity by dilantin has been reported (12, 18), and our work indicates that the tubulin binding activity of dilantin contributes to the combined drug effects on cells. *In vitro*, we find that the dilantin enhancement of the antimicrotubule effects of vinblastine is additive in terms of free energy. Dilantin at 400  $\mu\text{M}$  contributes about 117 ( $\pm 28$ ) cal/mol of unfavorable free energy to microtubule polymerization, both in the absence or presence of vinblastine (0.5–1.5  $\mu\text{M}$ ). By additivity, we mean there is a constant amount of unfavorable free energy within the thermodynamic cycle that is contributed by vinblastine and dilantin. This additivity implies the absence of cooperative interactions and suggests distinct binding sites and modes of microtubule inhibition.

What is the mechanism underlying the additivity of dilantin-vinblastine interactions with tubulin? In 2 M glycerol, 400  $\mu\text{M}$  dilantin has no effect on vinblastine-induced spiral size or on microtubule length. Two possible ways that dilantin may inhibit microtubule polymerization are by: (a) directly increasing microtubule catastrophe frequency; or (b) preferentially destabilizing microtubule ends. Microtubule dynamics studies investigating the mechanism of action of the tubulin

Table 4 Free energy for microtubule polymerization (PC-tubulin, 37°C)<sup>a</sup>

No podophyllotoxin	$\Delta\Delta G$	Podophyllotoxin
A. PC-tubulin	$\rightarrow$	500 nM podophyllotoxin
$\Delta G = -7.67 \times 10^3 \text{ cal/mol}$	$\Delta\Delta G = 210 \text{ cal/mol}$	$\Delta G = -7.46 \times 10^3 \text{ cal/mol}$
$\downarrow \Delta\Delta G = 270 \text{ cal/mol}$		$\Delta\Delta G = 250 \text{ cal/mol} \downarrow$
0.5 $\mu\text{M}$ vinblastine	$\rightarrow$	0.5 $\mu\text{M}$ vinblastine and
$\Delta G = -7.40 \times 10^3 \text{ cal/mol}$	$\Delta\Delta G = 190 \text{ cal/mol}$	500 nM podophyllotoxin
		$\Delta G = -7.21 \times 10^3 \text{ cal/mol}$
$\downarrow \Delta\Delta G = 170 \text{ cal/mol}$		$\Delta\Delta G = 190 \text{ cal/mol} \downarrow$
1 $\mu\text{M}$ vinblastine	$\rightarrow$	1 $\mu\text{M}$ vinblastine and
$\Delta G = -7.23 \times 10^3 \text{ cal/mol}$	$\Delta\Delta G = 210 \text{ cal/mol}$	500 nM podophyllotoxin
		$\Delta G = -7.02 \times 10^3 \text{ cal/mol}$
B. PC-tubulin	$\rightarrow$	1 $\mu\text{M}$ podophyllotoxin
$\Delta G = -7.67 \times 10^3 \text{ cal/mol}$	$\Delta\Delta G = 430 \text{ cal/mol}$	$\Delta G = -7.24 \times 10^3 \text{ cal/mol}$
$\downarrow \Delta\Delta G = 270 \text{ cal/mol}$		$\Delta\Delta G = 240 \text{ cal/mol} \downarrow$
0.5 $\mu\text{M}$ vinblastine	$\rightarrow$	0.5 $\mu\text{M}$ vinblastine and
$\Delta G = -7.40 \times 10^3 \text{ cal/mol}$	$\Delta\Delta G = 400 \text{ cal/mol}$	1 $\mu\text{M}$ podophyllotoxin
		$\Delta G = -7.00 \times 10^3 \text{ cal/mol}$

<sup>a</sup> The free energy was calculated from the  $K_p$ , equilibrium constant for microtubule polymerization, determined from turbidity experiments.  $\Delta G$  is the free energy for the addition of a tubulin heterodimer to a microtubule, and  $\Delta\Delta G$  is the change in free energy for microtubule polymerization due to the presence of podophyllotoxin, vinblastine, or both.

destabilizing protein oncoprotein 18/stathmin suggested that its mechanism of action is pH dependent (27). At pH 6.8, it sequesters tubulin in a 2:1 complex (tubulin: oncoprotein 18/stathmin), and at pH 7.5, it increases catastrophe frequency. The increase in catastrophe frequency was accompanied by a significant decrease in microtubule length beyond that which could be accounted for by sequestering tubulin heterodimers. By comparison, because microtubule lengths in the presence of dilantin are unchanged, it is not likely that dilantin increases microtubule catastrophe. "Endpoisoning" drugs, such as vinblastine, act at substoichiometric concentrations by preferentially destabilizing the microtubule minus ends (28). Because in addition plus ends are stabilized and rescue frequency is increased, this mechanism was shown to cause no alteration in average microtubule lengths. Given the weak affinity of dilantin for tubulin and the suprastoichiometric conditions required for dilantin activity, it seems unlikely that microtubule endpoisoning is the mechanism for the additive effect of dilantin. Furthermore, dilantin has no effect on vinblastine-induced tubulin spirals, indicating that the additive effect of dilantin is not mediated via an interaction with vinblastine-induced spirals at the microtubule end.

A third possible mechanism for the additivity of dilantin-vinblastine effects is simple sequestration of tubulin by dilantin in oligomers that do not participate in polymerization. In the sedimentation velocity studies, we looked for aggregate formation attributable to 400  $\mu\text{M}$  dilantin and found that at 37°C, there is a 2% increase in irreversibly aggregated protein, forming a sedimenting boundary at about 20–25S. This aggregated fraction is not large enough to account for the observed inhibition of microtubule polymerization, where the critical concentrations increase in the presence of dilantin by >20%.

To investigate whether tubulin heterodimer sequestration is a possible mechanism, we compared our results on combined dilantin-vinblastine energetics with podophyllotoxin-vinblastine energetics. Podophyllotoxin is known to sequester tubulin in a 1:1 complex with a  $K_d$  of 0.6–0.7  $\mu\text{M}$  (22). Unlike endpoisoning drugs such as Taxol and vinblastine, which are cytotoxic in cell culture at concentrations where microtubule mass is essentially unchanged, podophyllotoxin is cytotoxic at concentrations where microtubules depolymerize (29). Critical concentrations were determined for podophyllotoxin and podophyllotoxin-vinblastine combinations (data not shown). Table 4 gives the free energy changes calculated from the critical concentrations. It is noteworthy that the effects of podophyllotoxin, like dilantin, are additive, where 500 nM podophyllotoxin contributes about 200 cal/mol of unfavorable free energy to microtubule polymerization in the presence or absence of vinblastine, and in each cycle vinblastine contributes the same  $\Delta\Delta G$  in the presence or absence of podophyllotoxin. Likewise, 1  $\mu\text{M}$  podophyllotoxin and 0.5  $\mu\text{M}$  vinblastine contribute an equal amount of unfavorable  $\Delta\Delta G$  in the presence or absence of each other (Table 4B). These data, along with the observations that dilantin does not affect *Vinca*-induced tubulin spirals or microtubule lengths, suggest that dilantin acts like podophyllotoxin and sequesters tubulin in a nonpolymerizable 1:1 drug:tubulin complex.

The mechanism of action of podophyllotoxin, however, may not be completely analogous to that of dilantin. Microtubules formed *in vitro* in the presence of podophyllotoxin are shorter than in its absence (22). At substoichiometric drug concentrations, tubulin-GTP exchange at the microtubule ends is inhibited. This suggests that podophyllotoxin can affect the ends of microtubules either directly or indirectly by interacting near the microtubule ends, probably as a drug-tubulin complex. In our experiments, under steady-state conditions in 2 M glycerol, suprastoichiometric amounts of dilantin do not produce a significant difference in microtubule length compared with control experiments. Because there is a slight trend toward longer microtu-

bules (mean, 7.70 versus 7.36  $\mu\text{m}$ ), the addition of dilantin to a tubulin solution appears to affect microtubules in a way that is similar to a reduction in free tubulin concentration (30). Thus, our data support a mechanism whereby dilantin additivity in unfavorable free energy for microtubule polymerization occurs via sequestration of tubulin in 1:1 drug:tubulin complexes that do not participate in polymer formation. Although our data suggest this is the most likely mechanism, we cannot rule out the possibility that drug:tubulin complexes may interact very weakly with microtubules and not alter microtubule lengths significantly. Decreasing the pool of active tubulin alone would have an additive inhibitory effect on mitotic spindle growth, enhancing the antimitotic effectiveness of *Vinca* alkaloids.

The additive dilantin-vinblastine effects on microtubules *in vitro* clearly do not explain the synergy observed with dilantin and *Vincas* in cell culture (12, 18). Additional mechanisms involving proteins that destabilize microtubules or regulate cell cycle events are likely to be involved *in vivo*. Note that although drug synergy is often considered desirable, additivity also will enhance the clinical usefulness of these drugs. Our results do indicate combination drug therapies, where drugs act at a single receptor via different mechanisms, can be quantitatively investigated *in vitro* and demonstrated to have potential for enhanced efficacy. This type of drug-receptor data contributes to a quantitative understanding of combination chemotherapy and a rational selection of viable clinical therapies.

## ACKNOWLEDGMENTS

We thank Dr. Susan Wellman for critical reading of the manuscript. We also thank Pelahatchie Country Meat Packers for providing pig heads for tubulin purification.

## REFERENCES

1. Toso, R. J., Jordan, M. A., Farrell, K. W., Matsumoto, B., and Wilson, L. Kinetic stabilization of microtubule dynamic instability *in vitro* by vinblastine. *Biochemistry*, 32: 1285–1293, 1993.
2. Jordan, M. A., Thrower, D., and Wilson, L. Mechanism of inhibition of cell proliferation by *Vinca* alkaloids. *Cancer Res.*, 51: 2212–2222, 1991.
3. Lobert, S., Frankfurter, A., and Correia, J. J. Binding of vinblastine to phosphocellulose-purified and  $\alpha\beta$ -class III tubulin: the role of nucleotides and  $\beta$ -tubulin isotypes. *Biochemistry*, 34: 8050–8060, 1995.
4. Lobert, S., Vulevic, B., and Correia, J. J. Interaction of *Vinca* alkaloids with tubulin: a comparison of vinblastine, vincristine and vinorelbine. *Biochemistry*, 35: 6806–6814, 1996.
5. Lobert, S., Boyd, C. A., and Correia, J. J. Divalent cation and ionic strength effects on *Vinca* alkaloid-induced tubulin self-association. *Biophys. J.*, 72: 416–427, 1997.
6. Lobert, S., Ingram, J. W., Hill, B. T., and Correia, J. J. A comparison of the thermodynamic parameters for vinorelbine- and vinflunine-induced tubulin self-association by sedimentation velocity. *Mol. Pharmacol.*, 53: 908–915, 1998.
7. Lobert, S., and Correia, J. J. Antimitotics in cancer chemotherapy. *Cancer Nursing*, 15: 22–33, 1992.
8. Photiou, A., Shah, P., Leong, L. K., Moss, J., and Retsas, S. *In vitro* synergy of paclitaxel (taxol) and vinorelbine (navelbine) against human melanoma cell lines. *Eur. J. Cancer*, 33: 463–470, 1997.
9. Retsas, S., Mohith, A., and Mackenzie, H. Taxol and vinorelbine: a new active combination for disseminated malignant melanoma. *Anti-Cancer Drugs*, 7: 161–165, 1996.
10. Knick, V. C., Eberwein, D. J., and Miller, C. G. Vinorelbine tartrate and paclitaxel combinations: enhanced activity against *in vivo* P388 murine leukemia cell. *J. Natl. Cancer Inst.*, 87: 1072–1077, 1995.
11. Speicher, L. A., Barone, L., and Tew, K. D. Combined antimicrotubule activity of estramustine and taxol in human prostatic carcinoma cell lines. *Cancer Res.*, 52: 4433–4440, 1992.
12. Kawamura, K. I., Grabowski, D., Weizer, K., Bukowski, R., and Ganapathi, R. Modulation of vinblastine cytotoxicity by dilantin (phenytoin) or the protein phosphatase inhibitor okadaic acid involves the potentiation of anti-mitotic effects and induction of apoptosis in human tumour cells. *Br. J. Cancer*, 73: 183–188, 1996.
13. Rall, T. W., and Schleifer, L. S. Drugs effective in the therapy of the epilepsies. *In: A. G. Gilman, T. W. Rall, A. S. Nies, and P. Taylor (eds.), Goodman and Gilman's The Pharmacological Basis of Therapeutics*, Ed. 8, pp. 436–462. New York: Pergamon Press, 1990.
14. Burke, B. E., and Delorenzo, R. J.  $\text{Ca}^{2+}$  and calmodulin-regulated endogenous tubulin kinase activity in presynaptic nerve terminal preparations. *Brain Res.*, 236: 393–415, 1982.

15. MacKinney, A. A., Vyas, R. S., and Walker, D. Hydantoin drugs inhibit polymerization of pure microtubular protein. *J. Pharmacol. Exp. Ther.*, *204*: 189–194, 1978.
16. MacKinney, A. A., Vyas, R., Mueller, C., and Gorder, C. A comparison of potency of hydantoins in metaphase arrest and inhibition of microtubular polymerization. *Mol. Pharmacol.*, *17*: 275–278, 1980.
17. MacKinney, A. A., Jr., Vyas, R., and Mueller, C. 1-Acetyl-3-acetoxy-5'-5-diphenyl-hydantoin has colchicine-like activity against microtubular protein. *Res. Commun. Chem. Pathol. Pharmacol.*, *44*: 251–264, 1984.
18. Ganapathi, R., Hercbergs, A., Grabowski, D., and Ford, J. Selective enhancement of vincristine cytotoxicity in multidrug-resistant tumor cells by dilantin (phenytoin). *Cancer Res.*, *53*: 3262–3265, 1993.
19. Correia, J. J. Baty, L. T., and Williams, R. C., Jr.  $Mg^{2+}$  dependence of guanine nucleotide binding to tubulin. *J. Biol. Chem.*, *262*: 17278–17284, 1987.
20. Williams, R. C., Jr., and Lee, J. C. Preparation of tubulin from brain. *Methods Enzymol.*, *85*: 376–408, 1982.
21. Detrich, H. W., III, and Williams, R. C., Jr. Reversible dissociation of the  $\alpha\beta$  dimer of tubulin from bovine brain. *Biochemistry*, *17*: 3900–3907, 1978.
22. Schilstra, M. J., Martin, S. R., and Bayley, P. M. The effect of podophyllotoxin on microtubule dynamics. *J. Biol. Chem.*, *264*: 8827–8834, 1989.
23. Lee, J. C., Harrison, D., and Timasheff, S. N. Interaction of vinblastine with calf brain microtubule protein. *J. Biol. Chem.*, *250*: 9276–9282, 1975.
24. Liu, S., and Stafford, W. F., III. An optical thermometer for direct measurement of cell temperature in the Beckman Instruments XL-A analytical ultracentrifuge. *Ann. Biochem.*, *224*: 199–202, 1995.
25. Estus, S., and Blumer, J. L. Role of microtubule assembly in phenytoin teratogenic action in the sea urchin (*Arbacia punctulata*) embryo. *Mol. Pharmacol.*, *36*: 708–715, 1989.
26. Steel, G. G., and Peckham, M. J. Exploitable mechanisms in combined radiotherapy-chemotherapy: the concept of additivity. *Int. J. Radiat. Oncol. Biol. Phys.*, *5*: 85–91, 1979.
27. Howell, B., Larsson, N., Gullberg, M., and Cassimeris, L. Dissociation of the tubulin-sequestering and microtubule catastrophe-promoting activities of oncoprotein 18/stathmin. *Mol. Biol. Cell*, *10*: 105–118, 1999.
28. Panda, D., Jordan, M. A., Chu, K. C., and Wilson, L. Differential effects on vinblastine on polymerization and dynamics at opposite microtubule ends. *J. Biol. Chem.*, *271*: 29807–29812, 1996.
29. Jordan, M. A., Thrower, D., and Wilson, L. Effects of vinblastine, podophyllotoxin and nocodazole on mitotic spindles: implications for the role of microtubule dynamics in mitosis. *J. Cell Sci.*, *102*: 401–416, 1992.
30. Mitchison, T., and Kirschner, M. Dynamic instability of microtubule growth. *Nature (Lond.)*, *312*: 237–242, 1984.